Entanglement Distribution in LEO Satellite-based Dynamic Quantum Networks

Alena Chang, Yinxin Wan, Xuanli Lin, Guoliang Xue, Arunabha Sen

Abstract—**Recent advances in space quantum communications envision Low Earth Orbit (LEO) satellites for global entanglement distribution. Entanglement distribution in such a network requires considerations such as satellite mobility, ground station mobility due to the Earth's rotation, inter-satellite links, and multiple orbital shells, all of which have not been thoroughly studied in the networking literature. We ameliorate this deficit by defining a system model which accounts for all of the aforementioned factors. Using this system model, we formulate the dynamic optimal entanglement distribution (`DOED`) problem. We convert the `DOED` problem in a dynamic physical network to an instance of the problem in a static logical graph, the latter of which can be used to solve the former. We obtain a reduced logical graph from a logical graph, which can be used to reduce the complexity of solving the `DOED` problem. We propose two polynomial-time greedy algorithms for computing entanglement paths, as well as an integer linear programming (ILP)-based algorithm as a benchmark. We present evaluation results to demonstrate the advantages of our model and algorithms.**

1. Introduction

Low Earth Orbit (LEO) satellites offer a promising vehicle for global entanglement distribution [3], [8], [12], as they enable us to place repeaters, which facilitate end-to-end entanglement between two remote parties [13], in space. Under this architecture [4], [7], LEO satellites are partitioned into two categories based on their functionality: (1) entanglement sources, and (2) repeaters. Satellites of type (1) generate entangled photon pairs using entangled photon sources (EPSs) and transmit them to repeaters, while satellites of type (2) are armed with quantum non-demolition (QND) measurement devices and quantum memories (QMs) to perform entanglement swapping [2]. Ground stations carry QND and QM equipment as satellites of type (2) do. We henceforth refer to type (1) satellites as EPS satellites and type (2) satellites as QND-QM satellites. EPS satellites rely on *downlink channels* to transmit photons to ground stations and *inter-satellite links* to transmit photons to QND-QM satellites [12].

Distributing two-party entangled quantum states, or *ebits*, to two remote parties on Earth by way of satellites is far from a trivial task. The dynamic nature of the network due to satellite mobility and the Earth's rotation means the feasibility of photon transmission varies with time. If an EPS satellite generates an entangled photon pair and wishes to transmit these photons to two parties, which may be ground stations and/or QND-QM satellites, the EPS satellite must be within communication range of both parties, which may be the case at one point in time, but not the case at another point in time.

Alena Chang, Xuanli Lin, Guoliang Xue, and Arunabha Sen are affiliated with Arizona State University. Emails: {ahchang, xlin54, xue, asen}@asu.edu. Yinxin Wan is affiliated with UMass Boston. Email: Yinxin.Wan@umb.edu.
This research was supported by NSF grants 1663651, 2007083, and 2007469. The information reported herein does not reflect the position or the policy of the funding agencies.

Existing works on satellite-based entanglement distribution from a networking perspective include [1], [6], [9], [11], [14]. The work in [14] considers satellite mobility and allows entanglement distribution along inter-satellite links, but studies a small-scale example consisting of a chain of three satellites connecting two ground stations. The system model defined in [9] does not consider satellite and ground station mobility, while the system model defined in [6] does. Both [6] and [9] distribute entanglement exclusively using the double downlink configuration, in which an EPS satellite beams down an ebit to two ground stations, and do not permit entanglement distribution along inter-satellite links. The system models in both [1] and [11] take into account satellite mobility as well as entanglement distribution along inter-satellite links. All of [1], [5], [6], [11] assume constellations comprising equally spaced rings (circular orbits) of satellites in polar orbits, all at a single fixed altitude, akin to Iridium; while instrumental, current LEO satellite constellations like Starlink and Project Kuiper highlight the need to study entanglement distribution using constellations featuring inclined orbits.

To the best of our knowledge, a space-based entanglement distribution system model which incorporates satellite movement over time, ground station movement over time due to the Earth's rotation, inter-satellite links, and multiple orbital shells in inclined orbits at varying altitudes is absent in the literature. The main contributions of this paper are as follows.

- We propose a system model of an LEO satellite-based quantum network which considers satellite movement over time, ground station movement over time due to the Earth's rotation, entanglement distribution along inter-satellite links, and multiple orbital shells in inclined orbits at varying altitudes, with which we define the dynamic optimal entanglement distribution (`DOED`) problem.
- We expand on the concept of logical graphs as described in [1], which constructs the *static* logical graph corresponding to a *dynamic* physical network, by introducing the concept of a *reduced* logical graph, which we obtain from a given logical graph and can be used to reduce the complexity of solving the `DOED` problem.
- We design two polynomial-time greedy algorithms for solving the `DOED` problem.
- We conduct extensive performance evaluation to demonstrate the advantage of our system model and proposed algorithms, using an integer linear programming (ILP)-based algorithm as a baseline against which we study the performance of our greedy algorithms.

2. System Model

A. Physical System Definition

Together, LEO satellites and ground stations form the *nodes* of our physical network. While both QND-QM satellites and ground stations are equipped with the same hardware, we restrict entanglement swapping operations to QND-QM satellites so as to entirely eschew ground repeaters. If two ground stations Alice and Bob demand entanglement, we service their request solely using satellites. If a single EPS satellite is within communication range of both Alice and Bob, then the EPS satellite may transmit an ebit to the two parties. However, if the distance between Alice and Bob exceeds the communication range of a single EPS satellite, we require assistance from both EPS satellites and QND-QM satellites.

In this case, a chain of EPS satellites and QND-QM satellites in alternating order, with EPS satellites comprising the end nodes, can facilitate end-to-end entanglement between Alice and Bob. Each of the endmost EPS satellites distributes an ebit to one of Alice and Bob as well as a QND-QM satellite, while all other EPS satellites distribute ebits to two QND-QM satellites. The QND-QM satellites then perform entanglement swapping on their respective photons in QMs to extend entanglements as needed until Alice and Bob directly share an ebit. This approach uses the double downlink configuration, downlink/inter-satellite links, and double inter-satellite links.

We rely on a three-dimensional Cartesian coordinate system to define our physical network. The center of the Earth corresponds with the origin, the North and South poles form the positive and negative z-axes, respectively, and the equatorial plane coincides with the xy-plane. We assume the Earth is a sphere of radius $R_e = 6371$ km and takes 24 hours to complete a single rotation around the z-axis.

Our satellite constellation has L orbital shells. Each orbital shell $l = 0, 1, \dots, L-1$ comprises R_l rings, with each ring containing K_l satellites. Each ring is in inclined orbit, wherein every ring in an orbital shell l forms a nonzero angle γ_l with the equatorial plane, where $0 \le \gamma_l \le \pi/2$ is in radians.

A satellite $S_{l,r,k}$ is identified by its orbital shell $l = 0, 1, \dots, L-1$, its ring $r = 0, 1, \dots, R_l - 1$, and its index in the corresponding ring $k = 0, 1, \dots, K_l - 1$. All satellites in orbital shell l have the same altitude h_l (given in kilometers) and the same orbital period P_l (given in hours).

Say M ground stations populate our physical network, and they are indexed $g_i,\ i = 0, 1, \dots, M-1$. A ground station g_i is identified by its latitude $\phi_i,\ -\pi/2 \le \phi_i \le \pi/2$, and its longitude $\lambda_i,\ -\pi \le \lambda_i \le \pi$, both given in radians.

Each EPS satellite has a number of transmitters, while each QND-QM satellite/ground station has a number of receivers and QMs. The number of transmitters at a node restricts the number of ebits it can simultaneously transmit, while the number of receivers and QMs at a node restricts the number of ebits it can simultaneously receive and store, respectively. An EPS satellite can generate an ebit and use a transmitter to transfer a photon to a QND-QM satellite/ground station that is within communication range. The recipient node can then accept the photon using a receiver and store it in a QM. Successful photon transmission is heralded by the recipient node's QND measurement device.

Fig. 1 shows an example of the physical system we study.

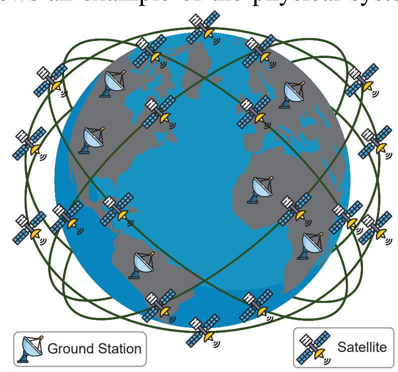

Fig. 1. An example of the type of network we study with 1 orbital shell comprising 6 rings and 6 satellites per ring.

B. Node Coordinates as a Function of Time

To define the position of satellite $S_{l,r,k}$ at time t (in hours), let orbital shell $l,\ 0 \le l \le L-1$, be arbitrary but fixed. We define a constant $\alpha_{l,r,k} = \frac{2\pi}{K_l} \times k$ ($r = 0, 1, \dots, R_l - 1, k = 0, 1, \dots, K_l - 1$) to equally distribute the K_l satellites on ring $r = 0, 1, \dots, R_l - 1$ in orbital shell l. We define another constant $\beta_{l,r} = \frac{2\pi}{R_l} \times r$ ($r = 0, 1, \dots, R_l - 1$) to equally distribute the R_l inclined rings in l around the z-axis.

Let a ring of radius $R_l = R_e + h_l$ lie on the xy-plane. Then the position of $S_{l,r,k}$ at time t is initially defined by $\vec{u}_{l,r,k}(t) = R_l(\cos(\frac{2\pi t}{P_l} + \alpha_{l,r,k}), \sin(\frac{2\pi t}{P_l} + \alpha_{l,r,k}), 0)^{\mathsf{T}}$. Rotate vector $\vec{u}_{l,r,k}(t)$ counterclockwise around the x-axis by γ_l radians using the rotation matrix $\mathbf{R}_x(\gamma_l)$ in order to obtain the desired inclined orbit. Using the coordinates produced by the matrix operation $\mathbf{R}_x(\gamma_l)\ \vec{u}_{l,r,k}(t)$, rotate them counterclockwise around the z-axis according to the corresponding ring r using the rotation matrix $\mathbf{R}_z(\beta_{l,r})$. Altogether, the position of satellite $S_{l,r,k}$ at time t is computed as $\vec{s}_{l,r,k}(t) = \mathbf{R}_z(\beta_{l,r})\mathbf{R}_x(\gamma_l)\vec{u}_{l,r,k}(t)$.

To define the position of ground station g_i at time t, let i be arbitrary but fixed. Given g_i's latitude ϕ_i and longitude λ_i, the position of g_i at time t is initially defined by $\vec{v}_{l,r,k}(t) = R_e(\cos\phi_i \cos\lambda_i, \cos\phi_i \sin\lambda_i, \sin\phi_i)^{\mathsf{T}}$. We depict the rotation of the Earth (counterclockwise around the z-axis) using the rotation matrix $\mathbf{R}_z(\frac{\pi t}{12})$. Altogether, the position of ground station g_i at time t is computed as $\vec{g}_i(t) = \mathbf{R}_z(\frac{\pi t}{12})\vec{v}_{l,r,k}(t)$.

C. Distance Between Two Nodes

The problem we study requires the Euclidean distance between two nodes, in particular the distance between two satellites as well as the distance between a satellite and a ground station. Let $d(t)$ denote the Euclidean distance between satellites $S_{l,r,k}$ and $S_{l',r',k'}$ at time t. Let $f(t)$ denote the Euclidean distance between satellite $S_{l,r,k}$ and ground station g_i at time t. Our problem study requires us to compute $\max_{t\in[\tau,\tau+\delta]} d(t)$ and $\max_{t\in[\tau,\tau+\delta]} f(t)$. We accomplish this end using approximation.

3. Modeling DOED Problem with Logical Graphs

A. Problem Formulation for Dynamic Physical Networks

The entanglement distribution problem we study entails delivering ebits to ground station pairs within a given time interval $[\tau, \tau+\delta]$ by way of satellite-assisted entanglement paths. Say we are given N connection requests $\mathcal{R} = \{r_0, r_1, \ldots, r_{N-1}\}$, all of which demand service as a batch within $[\tau, \tau+\delta]$. We define a connection request $r_i,\ i = 0, 1, \ldots, N-1$, as a 4-tuple (s_i, t_i, d_i, w_i), where s_i is the *source* node (a ground station), t_i is the *destination* node (another ground station), d_i is the non-negative integer *demand* which quantifies the number of ebits s_i and t_i wish to share, and w_i is the non-negative real *weight* associated with this request.

Successfully serving request r_i requires finding an s_i-t_i path π_i satisfying: (1) if the constituent nodes of π_i are s_i, v_0, v_1, $v_2, v_3, \cdots, v_{h-3}, v_{h-2}, v_{h-1}, v_h, t_i$, then $v_0, v_2, \ldots, v_{h-2}, v_h$ are EPS satellites, while $v_1, v_3, \ldots, v_{h-3}, v_{h-1}$ are QND-QM satellites; and (2) all of the constituent nodes of π_i have sufficient transmitters/receivers/QMs to support demand d_i.

Let $\mathcal{R}'$ be a subset of the connection requests $\mathcal{R}$. We say $\mathcal{R}'$ is *feasible* if (1) we can find a path π_i with sufficient transmitters/receivers/QMs to serve every $r_i \in \mathcal{R}'$ on the entire time interval $[\tau, \tau+\delta]$, and (2) for any two requests $r_i,\ r_j \in \mathcal{R}',\ i \neq j$, paths π_i and π_j do not share any transmitters/receivers/QMs. The total weight for serving a feasible $\mathcal{R}' \subseteq \mathcal{R}$ is $w(\mathcal{R}') = \sum_{r_i \in \mathcal{R}'} w_i$. The **Dynamic Optimal Entanglement Distribution** (DOED) problem seeks to find a feasible subset $\mathcal{R}_{opt}$ of $\mathcal{R}$ with maximum total weight.

B. Problem Formulation for Static Logical Graph

To solve the DOED problem, we construct a *static* logical graph corresponding to a given set of connection requests $\mathcal{R}$ from the *dynamic* physical network. We differentiate our logical graph from that in [5] by defining ours such that a node in our logical graph does not have a physical location, while a node in a logical graph defined using [5] has a physical location in that it may correspond to different satellites at different times.

Given $\mathcal{R}$ and $[\tau, \tau+\delta]$, we construct the corresponding logical graph $G = (V, E)$ as follows. For each node z (satellite/ground station) in the physical network, there is a corresponding vertex $l(z)$ in the logical graph. We use the notation $l(z)$ to indicate that *node* z in the physical network corresponds to *vertex* $l(z)$ in the logical graph. For each vertex v in the logical graph, there is a corresponding node $p(v)$ in the physical network. We use the notation $p(v)$ to indicate that *vertex* v in the logical graph corresponds to *node* $p(v)$ in the physical network.

Let $C_0 > 0$ be the inter-satellite communication range and let $C_1 > 0$ be the satellite-ground station communication range (both in kilometers). The constant C_0 denotes the maximum Euclidean distance at which an EPS satellite may beam a photon to a QND-QM satellite, while the constant C_1 denotes the maximum Euclidean distance at which an EPS satellite may beam a photon to a ground station.

We define the following two criteria to determine whether an edge exists between two vertices in the logical graph:

1) Let satellites $S_{l,r,k}$ and $S_{l',r',k'}$ be arbitrary but fixed. Let z and z' denote $S_{l,r,k}$ and $S_{l',r',k'}$ in the physical network, respectively. If $\max_{t\in[\tau,\tau+\delta]} d(t) \leq C_0$, then vertices $l(z)$ and $l(z')$ share an undirected edge in the logical graph.
2) Let satellite $S_{l,r,k}$ and ground station g_i be arbitrary but fixed. Let z and z' denote $S_{l,r,k}$ and g_i in the physical network, respectively. If $\max_{t\in[\tau,\tau+\delta]} f(t) \leq C_1$, then vertices $l(z)$ and $l(z')$ share an undirected edge in the logical graph.

We condense the two aforementioned criteria into a single criterion: For two vertices $u, v \in V$, there is an undirected edge $(u, v) \in E$ if and only if the *maximum distance between* $p(u)$ *and* $p(v)$ *in the interval* $[\tau, \tau+\delta]$ is within the communication range of $p(u)$ and $p(v)$. If $(u, v) \in E$ is an edge in the logical graph, we are guaranteed that $p(u)$ and $p(v)$ are within each other's communication range in the entire interval $[\tau, \tau+\delta]$. The number of transmitters/receivers/QMs at vertex $v \in V$ is the same as in $p(v)$.

Note that an edge $(u, v) \in E$ in the logical graph may only exist between an EPS satellite and a QND-QM satellite/ground station in the physical network due to their hardware. For two nodes in the physical network to be able to share an ebit (and hence share an edge in the logical graph), we require transmitters at one node and receivers/QMs at the other node.

The *bandwidth* of edge $(u, v) \in E$ is the number of ebits $p(u)$ and $p(v)$ can simultaneously support. If $p(u)$ is an EPS satellite and $p(v)$ is a QND-QM satellite/ground station, then the bandwidth of $(u, v) \in E$ is the *minimum* of the number of transmitters at $p(u)$, the number of receivers at $p(v)$, and the number of QMs at $p(v)$. If $p(v)$ is an EPS satellite and $p(u)$ is a QND-QM satellite/ground station, then the bandwidth of $(u, v) \in E$ is the *minimum* of the number of transmitters at $p(v)$, the number of receivers at $p(u)$, and the number of QMs at $p(u)$.

Now that we have established that the notion of a logical graph is well-defined, we *relax* our definition of feasibility from Section 3-A as follows. Let $\mathcal{R}'$ be a subset of the connection requests $\mathcal{R}$. We say $\mathcal{R}'$ is *feasible* if (1) we can find a path π_i with sufficient transmitters/receivers/QMs to serve every $r_i \in \mathcal{R}'$, and (2) for any two requests $r_i,\ r_j \in \mathcal{R}',\ i \neq j$, paths π_i and π_j do not share any transmitters/receivers/QMs. The total weight for serving a feasible $\mathcal{R}' \subseteq \mathcal{R}$ is $w(\mathcal{R}') = \sum_{r_i \in \mathcal{R}'} w_i$. Our relaxation manifests in criterion (1) in that we no longer have to consider whether the constituent links of a path π_i are operational in the entire time interval $[\tau, \tau+\delta]$, because the logical graph representation of the physical network frees us from this concern.

We henceforth study the DOED problem using our newly relaxed definition of a feasible $\mathcal{R}' \subseteq \mathcal{R}$.

C. Reduced Logical Graph

The number of edges in the logical graph can approach the order of $O((\sum_{l=0}^{L-1} R_l K_l + M)^2)$, potentially making the logical graph prohibitively expensive in terms of time complexity for the DOED problem. To ease the computational burden on our end, we introduce the notion of a *reduced logical graph*, which is a subgraph of the logical graph.

Given the logical graph corresponding with a set of connection requests $\mathcal{R}$ and time interval $[\tau, \tau+\delta]$, we construct the reduced logical graph by pruning vertices and edges from the logical graph using the following criteria.

1) Given a ground station z, if for any connection request $r_i \in \mathcal{R},\ i = 0, 1, \ldots, N-1$, z is not source node s_i or destination node t_i, we eliminate vertex $l(z)$ and any incident edges from the logical graph.
2) Given a satellite/ground station z, if for any connection request $r_i \in \mathcal{R},\ i = 0, 1, \ldots, N-1$, there exists no s_i-z path or z-t_i path with sufficient transmitters/receivers/QMs to support the demand d_i, we eliminate vertex $l(z)$ and any incident edges from the logical graph.

4. Computing Optimal Entanglement Distribution

A. ILP-Based Optimal Algorithm

We first design an Integer Linear Programming (ILP)-based algorithm that always computes the optimal entanglement distribution strategy. This can be used as a baseline in evaluation.

For each connection request $r_i \in \mathcal{R},\ i = 0, 1, \ldots, N-1$, define a binary indicator variable

$$\chi_i = \begin{cases} 1 & \text{if we serve connection request } r_i, \\ 0 & \text{if we do not serve connection request } r_i. \end{cases} \quad (1)$$

If $\chi_i = 1$, the transmitters/receivers/QMs corresponding to an s_i-t_i path π_i of bandwidth d_i are assigned to serve r_i.

Given the reduced logical graph, say $u \in V$ is an EPS satellite $p(u)$ in the physical network with T_u transmitters, while $v \in V$ is a QND-QM satellite/ground station $p(v)$ in the physical network with R_v receivers and Q_v QMs. We partition the vertices V of the reduced logical graph as follows: $V = \mathcal{S}_1 \cup \mathcal{S}_2 \cup \mathcal{G}$, where $\mathcal{S}_1$ denotes the EPS satellites, $\mathcal{S}_2$ denotes the QND-QM satellites, and $\mathcal{G}$ denotes the ground stations in the physical network. Using the indicator variables defined in Eq. (1) along with the newly defined set partition for V, we encapsulate the DOED problem as follows:

$$\textit{Objective}\text{: maximize} \sum_{i=0}^{N-1} w_i \cdot \chi_i \quad (2)$$

subject to the following constraints:

$$\chi_i \in \{0, 1\}, \qquad \forall i = 0, 1, \ldots, N-1 \quad (3)$$

$$\sum_{i=0}^{N-1} 2 \cdot d_i \cdot \chi_i \le T_z, \qquad \forall z \in \mathcal{S}_1 \text{ and } z \text{ in } \pi_i \quad (4)$$

$$\sum_{i=0}^{N-1} d_i \cdot \chi_i \le \min\{R_z, Q_z\}, \qquad \forall z \in \mathcal{G} \text{ and } z = s_i \text{ or } t_i \quad (5)$$

$$\sum_{i=0}^{N-1} 2 \cdot d_i \cdot \chi_i \le \min\{R_z, Q_z\}, \qquad \forall z \in \mathcal{S}_2 \text{ and } z \text{ in } \pi_i \text{ and } z \ne s_i \text{ and } z \ne t_i \quad (6)$$

To formulate the actual ILP-based optimal algorithm, we rely on entanglement flow as described in [10] to perform path computation. For each edge $(u, v) \in E$ in the reduced logical graph, we define $2 \times |E|$ binary indicator variables:

$$f_i(u, v) = \begin{cases} 1 & \text{if } r_i \text{ uses edge } (u, v) \in E, \\ 0 & \text{if } r_i \text{ does not use edge } (u, v) \in E, \end{cases} \quad (7)$$

and

$$f_i(v, u) = \begin{cases} 1 & \text{if } r_i \text{ uses edge } (v, u) \in E, \\ 0 & \text{if } r_i \text{ does not use edge } (v, u) \in E. \end{cases} \quad (8)$$

For $r_i \in \mathcal{R},\ i = 0, 1, \ldots, N-1$, we use $f_i(u, v)$ to quantify the amount of type-i flow from u to v and use $f_i(v, u)$ to quantify the amount of type-i flow from v to u.

Using the indicator variables defined in Eqs. (7) and (8), the overarching problem we seek to solve may be formulated as the following ILP problem:

$$\textit{Objective}\text{: maximize} \sum_{i=0}^{N-1} w_i \cdot \chi_i \quad (9)$$

subject to the following constraints:

$$\chi_i \in \{0, 1\}, \qquad \forall i = 0, 1, \ldots, N-1 \quad (10)$$

$$f_i(u, v) \in \{0, 1\}, \qquad \forall (u, v) \in E, i = 0, 1, \ldots, N-1 \quad (11)$$

$$\sum_{(s_i, v) \in E} f_i(s_i, v) - \sum_{(u, s_i) \in E} f_i(u, s_i) = \chi_i, \qquad \forall i = 0, 1, \ldots, N-1 \quad (12)$$

$$\sum_{(u, t_i) \in E} f_i(u, t_i) - \sum_{(t_i, v) \in E} f_i(t_i, v) = \chi_i, \qquad \forall i = 0, 1, \ldots, N-1 \quad (13)$$

$$\sum_{(u, z) \in E} f_i(u, z) = \sum_{(z, v) \in E} f_i(z, v), \qquad \forall i = 0, \ldots, N-1, z \in V, z \ne s_i \text{ and } z \ne t_i \quad (14)$$

$$\sum_{i=0}^{N-1} \sum_{(u, z) \in E} 2 \cdot d_i \cdot f_i(u, z) \le T_z, \qquad \forall z \in \mathcal{S}_1 \quad (15)$$

$$\sum_{i=0}^{N-1} \sum_{(z, v) \in E} d_i \cdot (f_i(z, v) + f_i(v, z)) \le \min\{R_z, Q_z\}, \qquad \forall z \in \mathcal{G} \text{ and } z = s_i \text{ or } t_i \quad (16)$$

$$\sum_{i=0}^{N-1} \sum_{(z, v) \in E} d_i \cdot (f_i(z, v) + f_i(v, z)) \le \min\{R_z, Q_z\}, \qquad \forall z \in \mathcal{S}_2 \text{ and } z \ne s_i \text{ and } z \ne t_i \quad (17)$$

Algorithm 1: W2D

Input: Logical graph $G(V, E)$ and the set of connection requests $\mathcal{R}$
Output: A feasible subset $\mathcal{R}_{W2D}$ of $\mathcal{R}$ and the service path π_i for each $r_i \in \mathcal{R}_{W2D}$

```
Sort the requests in R in non-increasing order of w_i/d_i. WLOG,
  assume that w_0/d_0 ≥ w_1/d_1 ≥ ··· ≥ w_{N-1}/d_{N-1};
R_W2D ← ∅;
for i := 0 to N − 1 do
    Compute an s_i-t_i path π_i of bandwidth at least d_i;
    Set π_i ← NULL if such a path does not exist;
    if π_i ≠ NULL then
        Add r_i to R_W2D;
        Reserve the resources needed for path π_i;
        Update graph G to its residual graph by removing the
          resources needed for path π_i;
Output R_W2D and {π_i | r_i ∈ R_W2D}.
```

B. Polynomial-Time Greedy Algorithms

Our greedy algorithms are presented in Algorithms 1 and 2. Algorithm 1 considers the requests in non-increasing order of the weight-to-demand ratio. Algorithm 2 considers the requests in non-increasing order of the weight-to-resources ratio. We quantify the resources required to satisfy a connection request r_i as the number of hops in a shortest s_i-t_i path π_i of bandwidth d_i (if such a path exists) multiplied by the bandwidth demand d_i. In both algorithms, whenever a request r_i can be served, the transmitters/receivers/QMs corresponding to the respective path π_i are reserved for r_i, and the available resources in the logical graph are updated accordingly.

Algorithms 1 and 2 each has a worst-case time complexity bounded by a lower-order polynomial. For Algorithm 1, after sorting, the main steps consist of N path finding processes. For Algorithm 2, the main steps consist of $O(N^2)$ path finding processes. While these algorithms are not guaranteed to find an optimal solution, they are very fast, and can find close to optimal solutions in most cases, as demonstrated in our evaluation results.

Algorithm 2: W2R

Input: Logical graph $G(V, E)$ and the set of connection requests $\mathcal{R}$
Output: A feasible subset $\mathcal{R}_{W2R}$ of $\mathcal{R}$ and the service path π_i for each $r_i \in \mathcal{R}_{W2R}$

$\mathcal{R}_{W2R} \leftarrow \emptyset$;
while TRUE **do**
  $ratio \leftarrow -\infty$; $index \leftarrow -\infty$;
  for $i := 0$ **to** $N - 1$ **do**
    if $r_i \notin \mathcal{R}_{W2R}$ **then**
      Compute an s_i-t_i path π_i of bandwidth at least d_i;
      Set $\pi_i \leftarrow$ `NULL` if such a path does not exist;
      if $\pi_i \neq \mathit{NULL}$ **then**
        $resources \leftarrow$ (hop count of π_i) $\times d_i$;
        if $w_i/resources > ratio$ **then**
          $ratio \leftarrow w_i/resources$; $index \leftarrow i$;
  if $ratio \neq -\infty$ **then**
    Add r_{index} to $\mathcal{R}_{W2R}$;
    Reserve the resources needed for path π_{index};
    Update graph G to its residual graph by removing the resources needed for path π_{index};
  else
    `break`
Output $\mathcal{R}_{W2R}$ and $\{\pi_i | r_i \in \mathcal{R}_{W2R}\}$.

5. Performance Evaluation

In this section, we present the evaluation results. The evaluation was done on a workstation running Ubuntu 22.04 system with i9-12900 CPU and 64GB memory. ILP instances were solved using the Gurobi optimizer.

A. Evaluation Settings

Physical Network: We use 60 ground stations, each located in a major city in the world. The satellite constellation contains $L = 1$ or 2 orbital shells. The first shell has an altitude of 550 km, an incline angle of 53°, and an orbital period of 1.5917 hrs. The second shell has an altitude of 570 km, an incline angle of 70°, and an orbital period of 1.5986 hrs. These parameters are drawn from the Starlink constellation. For each orbital shell, $R = K \in \{10, 20\}$. In a given ring, the EPS satellites and QND-QM satellites are arranged in alternating order. We take the inter-satellite communication range to be 3000 km and the satellite-ground station communication range to be 2000 km. The number of transmitters/receivers/QMs at a node is an integer between 5 and 10.

Connection Requests: The number of connection requests is $N = 10$ or 20. The source and destination nodes in each request are chosen from the 60 ground stations. The demand and weight for each request are integers between 1 and 5. We always take the start time to be $\tau = 0$ (midnight). We describe our choice of time interval length δ in Section (5-B).

B. Evaluation Scenarios

(i) In this scenario, we study 3 cases. In the first case, we let $L = 1, R = K = 10$. In the second case, we let $L = 1, R = K = 20$. In the third case, we let $L = 2, R = K = 20$. For each case, we generate 10 different sets of connection requests, each containing 20 requests where the source and destination nodes are randomly chosen from the 60 ground stations. The demand and weight for each request are random integers between 1 and 5. In all 3 cases, we let δ vary from 0.00 to 0.20 in increments of 0.01. This scenario is intended to study the impact of δ (for fixed L, R, K) in terms of average total weight.

(ii) In this scenario, we study 3 cases. In the first case, we let $L = 1, \delta = 0.01$. In the second case, we let $L = 1, \delta = 0.1$. In the third case, we let $L = 2, \delta = 0.1$. For each case, we generate 10 different sets of connection requests, each containing 20 requests, which are defined analogously as those in scenario (i). In all 3 cases, we let $R = K$ vary from 1 to 20 in increments of 1. This scenario is intended to study the impact of R and K (for fixed L, δ) in terms of average total weight.

(iii) In this scenario, we study 12 cases. With $R, K = 10$ fixed, for each value of $N = 10, 20$, $L = 1, 2$, and $\delta = 0.1, 0.01, 0.001$, we generate 100 different sets of connection requests: $\mathcal{R}_1^N, \mathcal{R}_2^N, \ldots, \mathcal{R}_{100}^N$. Each $\mathcal{R}_j^N$ contains N connection requests where the source and destination nodes are randomly chosen from the 60 ground stations, and the demand and weight are random integers between 1 and 5. This scenario is intended to evaluate the performance of the proposed greedy algorithms in terms of average running time for both the unreduced and reduced logical graphs, where the average is taken over $\mathcal{R}_j^N,\ j = 1, \ldots, 100$.

C. Evaluation Results

We present our evaluation results, along with our observations and analysis. We use `ILP`, `W2D`, and `W2R` to denote the ILP-based algorithm, Algorithm 1, and Algorithm 2, respectively.

Scenario (i): Fig. 2 illustrates the results of Scenario (i). Fig. 2(a) shows the impact of the value of δ on the total weight for $L = 1$ and $R = K = 10$. Fig. 2(b) shows the impact of the value of δ on the total weight for $L = 1$ and $R = K = 20$. Fig. 2(c) shows the impact of the value of δ on the total weight for $L = 2$ and $R = K = 20$. In all three sub-figures, the total weight computed by all three algorithms is non-increasing as the value of δ increases. This is because as the value of δ increases, fewer links will remain operational on $[\tau, \tau + \delta]$, and so the number of edges in the logical graph decreases. Despite this correlation, the value of δ beyond which servicing connection requests is no longer feasible is negligible in real-world implementations. For example, the maximum value of δ in Fig. 2 is 0.05 hours, or 3 minutes, which is ample time to establish an entanglement between two users in a quantum internet [8]. All three sub-figures show that the total weight computed by `W2D` and `W2R` is often suboptimal compared to that computed by `ILP`, but the greedy algorithms sacrifice optimality for efficiency, as mentioned in Section 4-B.

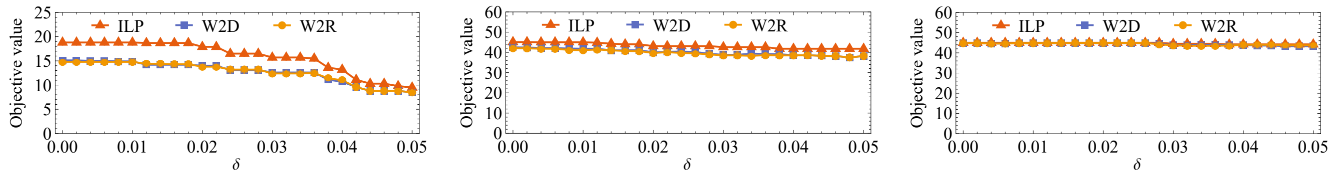

(a) $L = 1, R = K = 10$ (b) $L = 1, R = K = 20$ (c) $L = 2, R = K = 20$

Fig. 2. Performance of `ILP`, `W2D`, and `W2R` with varying values of δ.

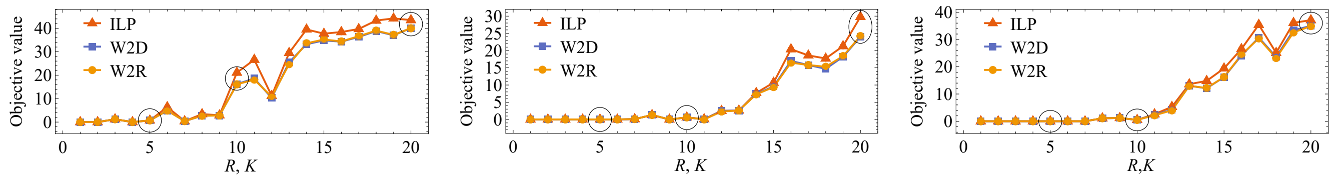

(a) $L = 1, \delta = 0.01$ (b) $L = 1, \delta = 0.1$ (c) $L = 2, \delta = 0.1$

Fig. 3. Performance of `ILP`, `W2D`, and `W2R` with varying values of R, K.

Scenario (ii): Fig. 3 illustrates the results of Scenario (ii). Fig. 3(a) shows the impact of the value of $R = K$ on the total weight for $L = 1$ and $\delta = 0.01$. Fig. 3(b) shows the impact of the value of $R = K$ on the total weight for $L = 1$ and $\delta = 0.1$. Fig. 3(c) shows the impact of the value of $R = K$ on the total weight for $L = 2$ and $\delta = 0.1$. We see that in all three sub-figures, the total weight computed by all three algorithms is non-decreasing (with some fluctuations) as the value of $R = K$ increases. The fluctuations can be attributed to the fact that as the value of $R = K$ increases, the number of edges in the logical graph does not necessarily increase as well. This is because the total weight is only guaranteed to be non-decreasing when R (and K) is increased to $n \times R$ (and $m \times K$) for any integers $n \geq 1$ (and $m \geq 1$). Increasing R (and K) to a multiple of itself produces a supergraph, or a "refinement", of the original logical graph. Fig. 3 illustrates this idea of refinement for $R = K = 5$, 10, and 20.

TABLE 1
AVERAGE RUNNING TIME OF `ILP`, `W2D`, AND `W2R` ALGORITHMS.

N	L	δ	Unreduced ILP Time	Reduced ILP Time	Reduced W2D Time	Reduced W2R Time
10	1	0.1	< 0.0001s	< 0.0001s	< 0.0001s	< 0.0001s
		0.01	0.0002s	0.0001s	< 0.0001s	< 0.0001s
		0.001	0.0002s	0.0001s	< 0.0001s	< 0.0001s
	2	0.1	0.0001s	< 0.0001s	< 0.0001s	< 0.0001s
		0.01	0.0006s	0.0003s	< 0.0001s	< 0.0001s
		0.001	0.0007s	0.0002s	< 0.0001s	< 0.0001s
20	1	0.1	< 0.0001s	< 0.0001s	< 0.0001s	< 0.0001s
		0.01	0.0002s	0.0002s	< 0.0001s	< 0.0001s
		0.001	0.0003s	0.0003s	< 0.0001s	< 0.0001s
	2	0.1	0.0002s	< 0.0001s	< 0.0001s	< 0.0001s
		0.01	0.0009s	0.0004s	< 0.0001s	< 0.0001s
		0.001	0.0016s	0.0005s	< 0.0001s	< 0.0001s

Scenario (iii): Table 1 presents evaluation results for the average running times for `ILP`, `W2D`, and `W2R`. We observe that `W2D` and `W2R` require much less time than `ILP`, which holds true in both the unreduced and reduced logical graphs. We also observe that in most of the cases, graph reduction helps to reduce the running time for `ILP`, `W2D`, and `W2R`.

6. CONCLUSION

In this paper, we propose a space-based global entanglement distribution model which considers satellite mobility, ground station mobility due to the Earth's rotation, inter-satellite links, and multiple orbital shells in inclined orbits. We also propose a rigorously defined scheme to compute entanglement paths for a set of connection requests such that all constituent links are guaranteed to be operational within a given time interval by obtaining a static logical graph from the dynamic physical network and then reducing it. We then design two polynomial-time greedy algorithms for solving the `DOED` problem.

REFERENCES

[1] A. Chang, Y. Wan, G. Xue, and A. Sen, "Entanglement distribution in satellite-based dynamic quantum networks," *IEEE Network*, vol. 38, no. 1, 2024.

[2] A. Chang and G. Xue, "Order matters: On the impact of swapping order on an entanglement path in a quantum network," in *Proc. of IEEE INFOCOM WKSHPS*, 2022.

[3] L. d. F. de Parny, O. Alibart, J. Debaud, S. Gressani, A. Lagarrigue, A. Martin, A. Metrat, M. Schiavon *et al.*, "Satellite-based quantum information networks: use cases, architecture, and roadmap," *Communications Physics*, vol. 6, no. 12, 2023.

[4] M. Gündoğan, J. S. Sidhu, V. Henderson, L. Mazzarella, J. Wolters, D. K. L. Oi, and M. Krutzik, "Proposal for space-borne quantum memories for global quantum networking," *npj Quantum Information*, vol. 7, no. 128, 2021.

[5] Y. Hu and V. O. K. Li, "Logical topology-based routing in leo constellations," in *Proc. of IEEE ICC*, 2001.

[6] S. Khatri, A. J. Brady, R. A. Desporte, M. P. Bart, and J. P. Dowling, "Spooky action at a global distance: analysis of space-based entanglement distribution for the quantum internet," *npj Quantum Information*, vol. 7, no. 4, 2021.

[7] C. Liorni, H. Kampermann, and D. Bruß, "Quantum repeaters in space," *New Journal of Physics*, vol. 23, no. 5, 2021.

[8] C.-Y. Lu, Y. Cao, C.-Z. Peng, and J.-W. Pan, "Micius quantum experiments in space," *Reviews of Modern Physics*, vol. 94, p. 035001, 2022.

[9] N. K. Panigrahy, P. Dhara, D. Towsley, S. Guha, and L. Tassiulas, "Optimal entanglement distribution using satellite based quantum networks," in *Proc. of IEEE INFOCOM WKSHPS*, 2022.

[10] M. Pant, H. Krovi, D. Towsley, L. Tassiulas, L. Jiang, P. Basu, D. Englund, and S. Guha, "Routing entanglement in the quantum internet," *npj Quantum Information*, vol. 5, no. 25, 2019.

[11] A. Sen, C. Sumnicht, S. Choudhuri, A. Chang, and G. Xue, "Quantum communication in 6G satellite networks: Entanglement distribution across changing topologies," in *Proc. of IEEE ICC*, 2024.

[12] J. S. Sidhu, S. K. Joshi, M. Gündoğan, T. Brougham, D. Lowndes, L. Mazzarella, M. Krutzik, S. Mohapatra *et al.*, "Advances in space quantum communications," *IET Quantum Communication*, vol. 2, no. 4, pp. 182–217, 2021.

[13] R. Van Meter, *Quantum Networking*. John Wiley & Sons, 2014.

[14] J. Wallnöfer, F. Hahn, M. Gündoğan, J. S. Sidhu, F. Wiesner, N. Walk, J. Eisert, and J. Wolters, "Simulating quantum repeater strategies for multiple satellites," *Communications Physics*, vol. 5, no. 169, 2022.